Thieme

Inhaled Treprostinil-Prodrug Lipid Nanoparticle Formulations Provide Long-Acting Pulmonary Vasodilation

Authors
Franziska G. Leifer[1,#,*], Donna M. Konicek[1,#,*], Kuan-Ju Chen[1], Adam J. Plaunt[1], Dany Salvail[2], Charles E. Laurent[2], Michel R. Corboz[1], Zhili Li[1], Richard W. Chapman[1], Walter R. Perkins[1], Vladimir S. Malinin[1]

Affiliations
1 Insmed Incorporated, Bridgewater, NJ, USA
2 IPS Therapeutique Inc., Sherbrooke, QC, Canada

Key words
Treprostinil, prodrug, lipid nanoparticle, pulmonary arterial hypertension, pharmacokinetics

received 22.09.2017
accepted 04.01.2018

Bibliography
DOI https://doi.org/10.1055/s-0044-100374
Published online: 23.5.2018
Drug Res 2018; 68: 605–614

ISSN 2194-9379

Correspondence
Vladimir Malinin, PhD
10 Finderne Ave
Building 10
Bridgewater, NJ 08807
Tel.: + 1/908/947 4334, Fax: + 1/908/526 4026
Vladimir.malinin@insmed.com

ABSTRACT

Treprostinil (TRE), a prostanoid analogue approved in the USA for the treatment of pulmonary arterial hypertension, requires continuous infusion or multiple dosing sessions per day for inhaled and oral routes of administration due to its short half-life. The inhaled drug is known to induce adverse systemic and local effects including headache, nausea, cough, and throat irritation which may be due at least in part to transiently high drug concentrations in the lungs and plasma immediately following administration [1]. To ameliorate these side effects and reduce dosing frequency we designed an inhaled slow-release TRE formulation. TRE was chemically modified to be an alkyl prodrug (TPD) which was then packaged into a lipid nanoparticle (LNP) carrier. Preclinical screening in a rat model of hypoxia-induced pulmonary vasoconstriction led to selection of a 16-carbon alkyl ester derivative of TRE. The TPD-LNP demonstrated approximately 10-fold lower TRE plasma C_{max} compared to inhaled TRE solution while maintaining an extended vasodilatory effect. The favorable PK profile is attributed to gradual dissociation of TPD from the LNP and subsequent conversion to TRE. Together, this sustained presentation of TRE to the lungs and plasma is consistent with a once- or twice-daily dosing schedule in the absence of high C_{max}-associated adverse events which could provide patients with an improved treprostinil therapy.

Abbreviations

CxTR	Abbreviation for treprostinil produg, where x represents the length of the attached alkyl chain (C2TR = ethyl treprostinil, C3TR = propyl treprostinil, etc.)
DP_1	Prostaglandin D2 receptor 1
IP	Prostacyclin receptor or prostaglandin I2 receptor
EP_1	Prostaglandin E2 receptor 1
EP_2	Prostaglandin E2 receptor 2
MMAD	Mass Median Aerodynamic Diameter
LNP	Lipid nanoparticle
PAH	Primary pulmonary arterial hypertension
TEM	Transmission Electron Microscopy
TPD	Treprostinil prodrug
TRE	Treprostinil

# These authors contributed equally to this work.
* Franziska G. Leifer and Donna M. Konicek are co-first authors.

Introduction

Pulmonary arterial hypertension (PAH) is a progressive disease characterized by increased pulmonary arterial pressure due to occluded and/or constricted pulmonary vasculature. Elevated pulmonary arterial pressure frequently overburdens the heart to the point of right ventricular hypertrophy, ventricular failure, and ultimately death [2, 3]. Even with current therapies, the 5 year survival rate of idiopathic PAH patients remains low at 65 % according to the US REVEAL registry [4].

There are several approved therapies to treat PAH, most of which aim to reduce pulmonary arterial pressure primarily through pulmonary vasodilation. Medications used to achieve this include prostaglandin receptor agonists (including prostacyclins, prostacyclin analogues, and IP receptor-specific agonists) [2, 5, 6], endothelin receptor antagonists [2, 5], phosphodiesterase inhibitors [2, 5], and

soluble guanylate cyclase activators[5]. Prostacyclin analogues, in particular, are attractive therapies due to their potent vasodilatory activity, ability to inhibit smooth muscle proliferation, and antiplatelet effects [2, 5, 7]. On the molecular level, the prostacyclin analogues iloprost and treprostinil bind strongly to cell-surface receptors on smooth muscle cells, including prostaglandin I2 receptor (IP) (both iloprost and treporostinil), prostaglandin E2 receptor 1 (EP_1) (iloprost only), and prostaglandin E2 receptor 2 (EP_2) and prostaglandin D2 receptor 1 (DP_1) (treprostinil only) [5, 7]. These receptors couple to stimulatory G proteins ($G_{\alpha s}$) to activate adenylate cyclase (AC), which produces cyclic AMP (cAMP) to alter intracellular calcium levels and induce vasodilation [4].

Currently, three prostacyclin analogues are approved to treat PAH in the US: epoprostenol, iloprost, and treprostinil (TRE) [2]. Epoprostenol was the first approved prostacyclin analogue on the US market; however, it has known chemical instability and demonstrates a short plasma half-life requiring continuous administration. Iloprost, administered by inhalation, also suffers from a short half-life and requires frequent dosing of 6 to 9 times daily [8]. TRE was developed as a more stable alternative [2]. Currently, TRE is available commercially as a continuous injection (Remodulin®), a solution for inhalation (Tyvaso®), and as an oral tablet (Orenitram®) [9]. Remodulin is administered by continuous infusion either intravenously (i. v.) or subcutaneously (s.c.), with each raising concerns (e. g., for line infection (i. v.) or infusion site pain (s.c.)) [9, 10]. While Tyvaso® provides local delivery to the lung, dosing is q.i.d. [1]. Although Orenitram® features the conveniences of oral administration it also requires repeated daily dosing (recommended b.i.d or t.i.d.) [11, 12]. Moreover, patients treated with Tyvaso and Orinetram experience adverse effects which are due to systemic exposure and in the case of Tyvaso, local adverse effects of cough and throat irritation [1, 12].

Here, we describe the development and preclinical evaluation of a sustained-release TRE formulation for delivery by inhalation. Our rationale was that by delivering drug directly to the lung with subsequent slow release of the active form the systemic adverse effects associated with high plasma C_{max} values could be reduced. Also, the airway exposure to active drug during inhalation would be reduced resulting in fewer adverse local effects. To achieve these goals, we synthesized a series of treprostinil prodrugs (TPDs) and packaged them into lipid nanoparticle (LNP) carriers. We characterized the in vitro conversion of TPD to TRE as a function of ester alkyl chain length and evaluated how it affected plasma concentrations of TRE in vivo. We confirmed efficacy using a cAMP activity assay in CHO-K1 cells and using a hypoxia-induced rat model of pulmonary arterial vasoconstriction.

Materials and Methods

Ethical conduct

The treatment of all animals used in these studies was conducted per the Canadian Council on Animal Care (CCAC) guidelines. The experimental protocols for rat in vivo studies were approved by the CCAC Committee at IPS Therapeutique Inc., Sherbrooke, Quebec, Canada; Rat, dog, and monkey lung tissues for in vitro prodrug conversion studies were provided by ITR Laboratories Canada, Montreal, Quebec, Canada. All experiments involving animals were carried out in compliance with the 'Guide for the Care and Use of Laboratory animals' published by the National Academy of Sciences.

Materials

Treprostinil was obtained from Chirogate International (Taoyuan, Taiwan). Propanol, butanol, pentanol, hexanol, octanol, decanol, dodecanol, tetradecanol, hexadecanol, 1,4 dioxane, amberlyst-15 resin, acetonitrile, formic acid, trimethylamine, squalane, and methanol were acquired from Sigma (St. Louis, MO, USA). Cholesterol conjugated to polyethyleneglycol 2000 MW (Chol-PEG 2000) was acquired from NOF America (White Plains, NY, USA). 1,2-dioleoyl-sn-glycero-3-phosphocholine (DOPC) was acquired from Avanti Polar Lipids (Alabaster, Alabama, USA). Ethyl Alcohol, 200 Proof was acquired from Pharmco Aaper (Brookfield, CT, USA). Phosphate buffered saline (PBS) was acquired from Mediatech (Manassas, VA, USA).

Treprostinil prodrug synthesis

A small library of TPDs was prepared via esterification of treprostinil acid catalyzed by the acidic resin Amberlyst-15. Briefly, treprostinil acid and linear alcohols of various alkyl chain length were combined in a 1:10 molar ratio in the presence of 1,4-dioxane; dioxane was omitted for short chain alcohols that were a liquid at room temperature. Amberlyst-15 resin was then added to the treprostinil/alcohol mixture to catalyze the esterification reaction (1 g resin per 40 mg TRE). The reaction mixture was placed on an incubated shaker (MaxQ 4450, ThermoFisher Scientific, Waltham, MA, USA) set to 50 rpm and 40 °C for ~14 h. A solid-liquid extraction using acetonitrile was used to remove the desired product from the resin catalyst. Crude product was purified using preparatory high-performance liquid chromatography (HPLC) (100 × 21.2 mm ACE CN 5 µm column) to yield the desired products (typically thick colorless oils for short chain TPD or white waxy solids for longer chain TPDs). ^{1}H and ^{13}C NMR structural characterization was performed for all synthesized compounds to confirm their identity. Purity was confirmed by HPLC-UV.

TPD to TRE conversion in lung tissue homogenate

Study was performed at ITR Laboratories (Montreal, Canada). Lung tissue was retrieved from healthy animals and homogenized with PBS at 1:5 tissue: PBS ratio. Lungs were used from Sprague Dawley rats, Beagle dogs, and Cynomolgus monkeys. Total protein concentration was adjusted to 10 mg/mL and a 10 µM stock solution of TPD or TRE in DMSO was added into a 1 mL lung homogenate to achieve a final concentration of 200 nM. The mixture was incubated at 37 °C for 0.25, 0.5, 1, 2, and 4 h. Post incubation, TPD and TRE were extracted using acetonitrile with 1 % formic acid and quantified by HPLC/MS/MS. 1-Naphthoxyacetic Acid was used as an internal standard. The rate of TPD conversion was determined as the slope at zero time using nonlinear exponential regression (1 phase association) of all data points by GraphPad Prism.

TPD-LNP manufacturing

TPD-LNPs were made using a proprietary alcohol injection procedure for the one-step production of monodisperse nanoscale TPD-LNPs. A center stream of alcohol-solvated lipid containing TPD,

squalane, DOPC, and Cholesterol-PEG 2000 was impinged with adjacent streams of aqueous buffer positioned perpendicular to the lipid feed line in a mixing cross. As prodrugs and lipid excipients diffused from the alcohol stream into surrounding aqueous buffer (antisolvent), they began to precipitate, facilitating the spontaneous formation of nanoscale TPD-LNPs. By controlling the magnitude and relative ratios of the TPD-LNP precursor flow inputs, the particle size and size uniformity of the product were easily and reproducibly tuned.

TPD-LNP particle size characterization

Particle size characteristics were determined by dynamic light scattering (DLS) using a Wyatt Technology Mobius (Wyatt Technologies, Santa Barbara, CA, USA) fitted with a disposable microcuvette insert. Dynamics® software (Wyatt Technologies, Santa Barbara, CA, USA) was used for data acquisition and analysis.

TPD-LNP Imaging by Cryo-TEM

To prepare cryo-TEM grids, 2.5 µL of sample was applied to a Quantifoil grid, blotted for 15 s with an FEI vitrobot in 100 % humidity, and then plunged into liquid ethane. The image was collected on a FEI Tecnai TF20 at an accelerating voltage of 200 kV using TVIPS EM-Menu program. The instrument is equipped with a 16-megapixel CCD camera. The nominal magnification used was 50,000 x with 2 binning. These studies were performed at the Electron Imaging Center for NanoMachines and CNSI of the University of California, Los Angeles (UCLA). The center is supported by NIH (1S10RR23057 to ZHZ).

HPLC assay

TRE, TPD, and excipient concentrations were analyzed on a Waters Alliance 2695 separations module connected to a photodiode array (PDA) (Waters Corporation, Milford, MA, USA) to measure the absorbance of TRE and TPDs at 272 nm and a charged aerosol detector (CAD) (Thermo Fisher Scientific, Waltham, MA, USA) to measure the concentration of excipients. A gradient method was used for separation of the TRE, TPD, and excipients: mobile phase A (acetonitrile 25 %, methanol 25 %, water 50 %, formic acid 0.1 %, triethylamine 0.01 %) and B (acetonitrile 50 %, methanol 50 %, formic acid 0.1 %, triethylamine 0.01 %), where B increased from 40 % to 50 % from 0 to 2 min, then to 75 % by 3 min, 95 % by 11 min, and 100 % by 13 min. Mobile phase B remained at 100 % until 17 min and returned to 40 % at 17.5 min. The flow rate was 1 mL/min and the assays were run at room temperature.

cAMP assay

CHO-K1 cells (ATCC® CCL-61) were transiently co-transfected with pGloSensor™ -22 F cAMP plasmid (Promega, Madison, WI, USA) and prostanoid receptor (EP_2) plasmid (Origene, Rockville, MD, USA). Transfected cells were treated with 5 µM of either TRE or TPD-LNP up to 4 h. cAMP levels were measured every 5 min for the duration of the studies using a Synergy Neo plate reader (BioTek, Winooski, VT, USA) and the increase in cAMP activation was calculated relative to vehicle control. Each formulation was tested in 3 or 4 individual runs and the rate (slope) of cAMP activation was determined using linear regression of all data points during first 180 min for LNP formulations and 120 min for the micellar formulation by GraphPad Prism.

Plasma Pharmacokinetics (PK)

Plasma PK experiments in anesthetized ventilated rats were performed as follows: nebulized TRE solution and TPD formulations at a volume of 250 µL were administered over a period of approximately 1 min at 15 nmol/kg (6 µg/kg TRE equivalent) to anesthetized male Sprague Dawley rats prepared with an endotracheal tube for ventilation. The right femoral vein was cannulated to facilitate blood collections at specified time points. Terminal lung samples were taken for analysis 6 h after dosing. An Aeroneb® nebulizer and a controller (Aerogen, Galway, Ireland) were used to produce an aerosol of a mass median aerodynamic diameter (MMAD) of around 2.4 µm at a sampling rate of 2 L/min. A SAR-830/AP Small Animal Ventilator (CWE Inc., Ardmore, PA) set at a ventilator tidal volume (VT) of 8 mL/kg and respiratory rate of 90 breaths/min, was used to deliver nebulized test articles. Blood and lung tissue samples were taken at selected times after nebulization of the drugs. TRE and TPD concentrations in blood plasma and lung tissue were quantified by HPLC/MS/MS analysis.

PAP measurements

Male Sprague Dawley rates were anesthetized, artificially ventilated, and prepared for measurement of mean pulmonary arterial pressure (mPAP), systemic blood pressure (mSAP), heart rate (HR), and arterial oxygen saturation (SaO_2). Specifically, a catheter was surgically placed into the right femoral artery to monitor the arterial pressure throughout the procedure and a tracheotomy was performed to introduce an endotracheal tube to allow the animals to be mechanically ventilated and monitored. Pilot studies were performed to find the optimum volume (3.5–4 mL) for mechanical ventilation and fixed at a volume that produced a 10–15 cm H_20 pulmonary inflation pressure for a 300–350 g rat. Following a sternotomy, the pericardium was opened to introduce a 20-gauge catheter into the root of the pulmonary artery for the measurement of pulmonary arterial pressure. Physiologic parameters were measured during normoxia (fraction of inspired oxygen [FIO_2] = 0.21, $SaO_2 \approx 90$ %) and for 2 to 3 h during hypoxia ($FIO_2 = 0.10$, $SaO_2 \approx 50$ %). Compounds were delivered via the Aeroneb® (Aerogen, Galway, Ireland) nebulizer interposed in a ventilator circuit at an estimated pulmonary dose of 6 µg/kg [13]. A total of 250 µL test article was nebulized over a period of approximately 1 min, starting 10 min after inducing hypoxia.

TRE and TPD assay in lung homogenate and plasma samples

TRE and TPD were measured in plasma PK samples and lung homogenate ex vivo samples by LC/MS/MS assays. The TRE assay had a lower limit of quantitation (LLOQ) of 25 pg/mL in rat plasma and 250 pg/mL in lung homogenate. The TPD assay had a LLOQ of 100 pg/mL in rat plasma and 300 pg/mL in lung homogenate. Briefly, TRE and TPD were extracted from plasma and lung homogenate samples by liquid extraction in acetonitrile/water/acetic acid (50/50/0.5, v/v/v). 1-Naphthoxyacetic Acid was used as an internal standard for TRE and hexadecyl TRE (C16TR) was used as an internal standard for octyl TRE (C8TR), decyl TRE (C10TR), dodecyl TRE

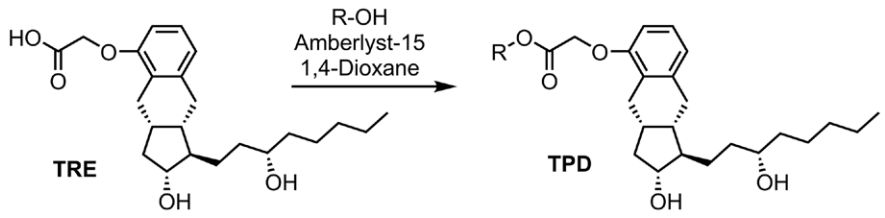

▶ **Fig. 1** Reaction scheme for the acid-catalyzed esterification of treprostinil (TRE) used to form alkyl ester treprostinil prodrugs (TPD). R = CH_2CH_3 through $(CH_2)_{15}CH_3$.

(C12TR), and tetradecyl TRE (C14TR) TPDs. Extracts were analyzed using Ace 3 C18 (Kinetex Phenyl-Hexyl, Phenomenex, Torrance, CA, USA) reverse phase analytical column at a flow rate of 1 mL/min. The gradient method was used with Mobile Phase A prepared as 1 % formic acid in water and Mobile Phase B as 100 % Acetonitrile. The starting concentration of Mobile Phase B in the gradient was 35 %. Detection was done by tandem mass spectrometry (AB SCIEX API 4000, Framingham, MA, USA).

PK data analysis

For studies in anesthetized rats, blood samples were obtained at 3, 30, 60, 120, 240, and 360 min from the start of nebulization. The following PK measurements were made: mean maximum concentration (C_{max} (ng/mL), time to maximum plasma concentration (T_{max} (min)), and area under the curve ($AUC_{0\text{-}6h}$ or $AUC_{0\text{-}24}$ (ng * h/mL)) calculated by the trapezoid method [14].

Statistical methods

Nonlinear and linear regression analysis including determination of confidence intervals and standard deviation was performed using the GraphPad Prism 6 software package (GraphPad Software Inc., La Jolla, CA). Statistical analysis of C_{max} values was performed using 1-way ANOVA with Tukey's multiple comparison test and post test for linear trend analysis.

Results

TPD synthesis and characterization

TPD synthesis was carried out by esterification of TRE in the presence of alcohol to yield alkyl ester derivatives with chain lengths ranging from ethyl (C_2H_5) to octadecyl ($C_{18}H_{37}$). A schematic of TPD synthesis is shown in ▶ **Fig. 1.** Reaction of TRE with alcohols of varying chain length in the presence of an acid resin catalyst yielded a crude product that was purified using preparatory HPLC to remove reaction impurities. Structural characterization of select TPDs was confirmed using ^{1}H NMR, ^{13}C NMR, and mass spectrometry (see Methods and **Table S1**). Typical purity by HPLC-UV was not less than 97 %.

TPD-LNP formulation

TPD-LNPs were prepared using a proprietary process (▶ **Fig. 2a**). TPDs with alkyl chain length of 10 carbons or longer have progressively lower water solubility and can be efficiently dosed as a suspension of nanoparticles. We designed stable nanoparticles with a high load of prodrug (30 % wt/wt) composed of TPD, the hydrocarbon squalane, the phospholipid DOPC, and the PEGylated lipid Cholesterol-PEG 2000. TPD and squalane, together constituting 80 mol % of the nanoparticle, are believed to form a hydrophobic core, while amphiphilic DOPC and Cholesterol-PEG 2000 occupy LNP surface and stabilize nanoparticles. The process is attractive also as it can be adapted readily for larger scale production.

Further optimization by varying nanoparticle composition and process parameters yielded nanoparticles with an average size of 100 nm. A representative TEM micrograph of TPD-LNPs is shown in ▶ **Fig. 2b**. The size of the solid lipid nanoparticles visible on the TEM micrograph is in agreement with DLS size measurement data shown in **Fig. S1**.

Delivery to the lung of TPD-LNPs was done as an aqueous aerosol generated by nebulization using an Aeroneb® nebulizer. The mean median aerodynamic diameter (MMAD) of the aerosol droplets was measured using the Marple impactor to be approximately 2.4 µm for all formulations investigated (**Fig. S2** and **Table S2**) [15]. We tested and confirmed that nebulization did not significantly affect the nanoparticle size and did not change the association of TPD to nanoparticles. The particle size of aerosolized LNPs that were reclaimed by condensation using a chilled impinger was changed by not more than 30 %.

TPD stability in vitro and ex vivo

To further characterize the TPDs, both spontaneous hydrolysis and enzyme-mediated conversion (de-esterification) of the prodrug to the therapeutically-active TRE were evaluated. Both rates of conversion were determined to be inversely proportional to TPD chain length, i.e the longer the TPD chain length the slower the TPD to TRE conversion rate. No measurable spontaneous hydrolysis was observed for TPDs with alkyl chain lengths greater than C6TR and no measurable enzyme conversion was observed for C16TR under the conditions tested (**Fig. S3a and b**).

Ex vivo TPD to TRE conversion was assessed for C8TR – C14TR in rat lung homogenate and for C8TR - C12TR in dog and monkey lung homogenate. In agreement with the observations from the esterase-mediated conversion investigations, TPD to TRE conversion was chain-length-dependent (▶ **Fig. 3a**), with the initial rate of conversion in rats ranged from 188 %/h for C8TR to 1.1 %/h for C14TR. The conversion rate varied in lung tissue homogenates from different species as shown for C12TR in ▶ **Fig. 3b.** For C8TR – C12TR

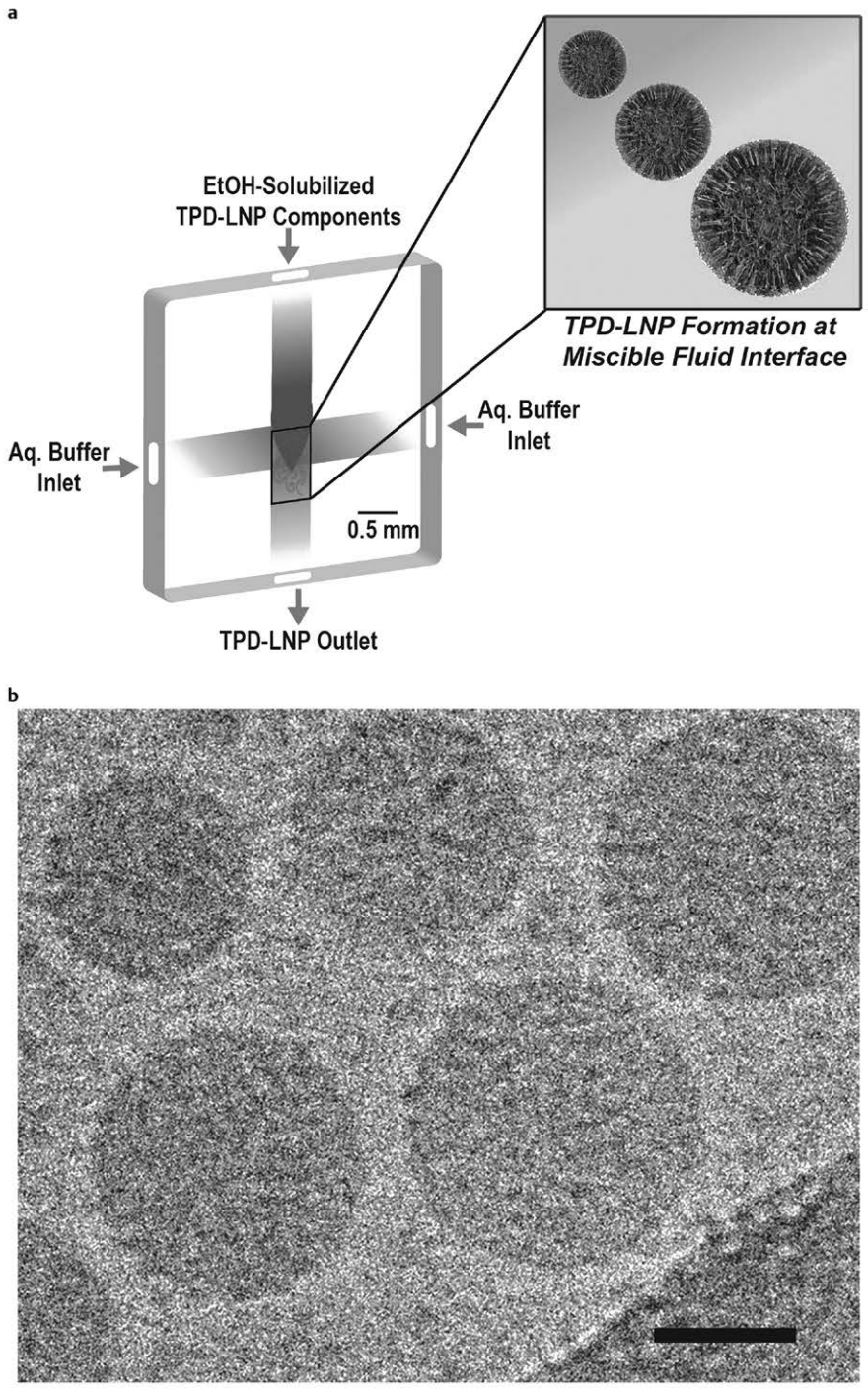

▶ **Fig. 2** Schematic representation of manufacturing process **a** and cryo-transmission electron microscopy (TEM) of hexadecyl treprostinil solid lipid nanoparticles (C16TR-LNP) Scale bar = 40 nm **b**.

the conversion rates decreased in the order dog > rat > monkey (▶ **Table 1**).

TPD-LNP activity in vitro

An in vitro pGloSensor assay was utilized to monitor cAMP production kinetics in CHO-K1 cells co-transfected with the EP_2 receptor and pGloSensor-22 F plasmids over time in the presence of TRE versus TPD-LNPs (▶ **Fig. 4**). TRE initiated a rapid spike in cAMP production to 16-fold of baseline within the first 20 min of exposure, after which it declined and reached a steady state of ~12-fold cAMP levels after 90 min. In contrast, cells treated with C10TR to C16TR TPD-LNPs exhibited slower-developing cAMP generation to approximately 10-, 7-, 6-, and 4-fold of baseline, respectively, over the course of approximately 180 min (▶ **Fig. 4a**). The average slopes

of the cAMP productions during the first 180 min were 0.050 (0.003), 0.037 (0.002), 0.021 (0.001), and 0.017 (0.0015) fold/min for C10TR-LNP, C12TR-LNP, C14TR-LNP and C16TR-LNP, respectively. The numbers in parenthesis show the standard error corresponding to a 95 % confidence interval for the slope. In general, longer prodrug chains yielded a slower increase of cAMP production, an indicator of TPD to TRE conversion. This observation was in agreement with those from cell-free and lung tissue homogenate studies. To investigate whether the LNP formulation provided any benefit for the kinetics of TRE release, cAMP production kinetics of C12TR-LNP and its micellar counterpart (C12TR-Micelle) were compared in CHO-K1 cells using the same pGloSensor assay. As shown in ▶ **Fig. 4b,** the C12TR-LNP exhibited a slower-developing effect with a slope of 0.037 compared to C12TR-M, which has a steeper slope of 0.056 (0.003) folds/min and peaked at 120 min vs the LNP's 180 min, demonstrating an advantage to the LNP vehicle in delaying presentation of the TPD and subsequent TRE to the cell milieu.

PK of TRE and TPD administered by inhalation

To assess whether the chain-length-dependent conversion of TPD to TRE and the sustained release of TRE from TPD-LNPs observed in vitro is also reflected in vivo, plasma levels of TRE were measured over a 6 h period in anesthetized, ventilated rats that were treated with inhaled TRE, TPD-LNP, or micellar TPD (TPD-M) (▶ **Fig. 5**). A micelle form was included as it provided a dynamic formulation from which TPD would be more readily available for the lung esterases (note that TPD is not soluble in solution and therefore a vehicle is required to allow suspension). TRE generated the highest plasma C_{max} (3.4 ng/mL) observed immediately post-dose and was eliminated from the plasma below level of quantitation after 4 h. Ventilated rats treated with inhaled TPD-LNPs of C12TR, C14TR, and C16TR had plasma TRE C_{max} values of 0.56, 0.35, and 0.22 ng/mL, respectively (▶ **Fig. 5a** and ▶ **Table 2**), all were statistically different from TRE C_{max} as determined by 1-way ANOVA analysis. A significant linear trend of decreasing C_{max} ($p = 0.002$, Post test for linear trend) was observed for increasing TPD alkyl chain lengths. The t_{max} was observed at 0.05 h for TRE compared to 0.5 h for both C12TR and C14TR and at 1 h for C16TR (▶ **Table 2**). After inhalation of TPD-Micelle plasma levels of TRE were 3 – 4 times higher ($p < 0.05$) (2.4, 1.20, and 0.84 ng/mL for C12TR, C14TR, and C12TR, correspondingly) than with TPD-LNP (▶ **Fig. 5b** and ▶ **Table 2**), consistent with earlier in vitro observations.

In vivo effects

In vivo effects of TRE and TPD-LNPs were compared by measuring reduction of pulmonary arterial pressure (PAP) in a hypoxic pulmonary vasoconstrictive rat model simulating the increased pulmonary pressure characteristic of PAH (▶ **Fig. 6**). Normoxic baseline PAP in rats ventilated with normal air varied between rats with an average value of 18.4 mmHg and a standard deviation of 2.2 mmHg. Hypoxia induced by a gas mixture with reduced oxygen level (10 %) produced increases in PAP to an average 24.2 mmHg (SD = 2.8 mmHg). After the elevated PAP stabilized, rats were dosed by inhalation. To compare the effect of inhaled test articles, the PAP values were normalized to the hypoxic baseline for each rat. With that scaling, the hypoxic PAP equals 100 %, while the average normoxic baseline PAP is 76 %. Inhaled TRE resulted in an immediate post-dose reduction of PAP to approximately 70 % (slightly below normoxic baseline) that returned to hypoxic baseline levels

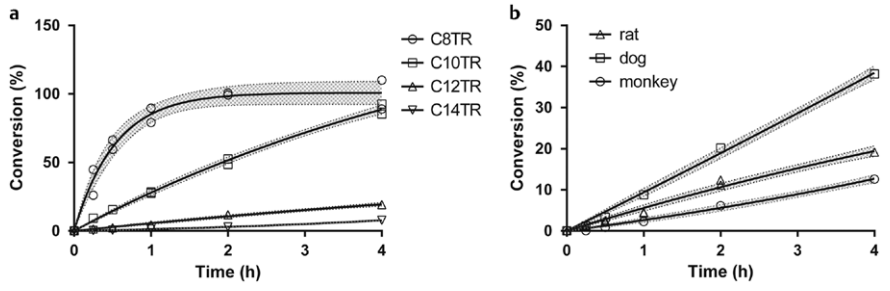

▶ **Fig. 3** Conversion of treprostinil prodrugs (TPDs) with increasing alkyl chain length to treprostinil (TRE) in lung tissue homogenate as a function of time: **a** in the presence of rat lung tissue homogenate and **b** Conversion rates of dodecyl TRE (C12TR) to TRE in rat, dog, and monkey lung tissue homogenates. Value at each time point is an average of n = 2 individual samples. Fitted lines are obtained from exponential regression (1 phase association in GraphPad Prism) and shaded areas represent 95 % confidence interval of the slope.

▶ **Table 1** Conversion rates of treprostinil prodrugs in rat, dog, and monkey lung homogenate.

Rate of TPD Conversion (%/h)	C8TR	C10TR	C12TR	C14TR
Rat	187.6 (18.6)	30.3 (1.35)	5.85 (0.48)	1.13 (0.026)
Dog	313.4 (25.7)	62.0 (5.35)	9.31 (0.57)	NM
Monkey	86.5 (7.63)	19.9 (1.48)	2.48 (0.30)	NM

The rate of TPD conversion was determined as the slope at zero time using nonlinear exponential regression (1 phase association) of all data points (0, 0.25, 0.5, 1, 2, and 4 h) measured in duplicates by GraphPad Prism. Standard Error representing 95 % confidence interval is shown in parenthesis.
NM – not measured.

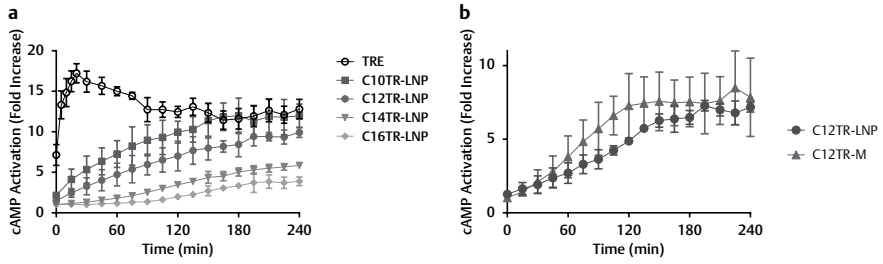

▶ **Fig. 4** Kinetics of cyclic AMP (cAMP) activation in CHO-K1 cells co-transfected with prostaglandin E2 receptor 2 (EP_2) /pGloSensor-22 F plasmids in the presence of free treprostinil (TRE) vs. treprostinil prodrug lipid nanoparticles (TPD-LNP) (5 µM) **a** and dodecyl TRE-LNP (C12TR-LNP) vs. C12TR-Micelle (C12TR-M) **b**) Kinetics were measured every 5 min, but every 15 min is shown for clarity. Each time point represents an average value of 3 or 4 runs, with error bars showing SD. The average slopes (with the standard error of the slope) of the cAMP productions induced by TPD-LNPs during first 180 min were 0.050 ± 0.003, 0.037 ± 0.002, 0.021 ± 0.001, and 0.017 ± 0.0015 fold/min for C10TR-LNP, C12TR-LNP, C14TR-LNP and C16TR-LNP, respectively. C12TR-M induced slope during first 120 min was 0.056 ± 0.003 fold/min.

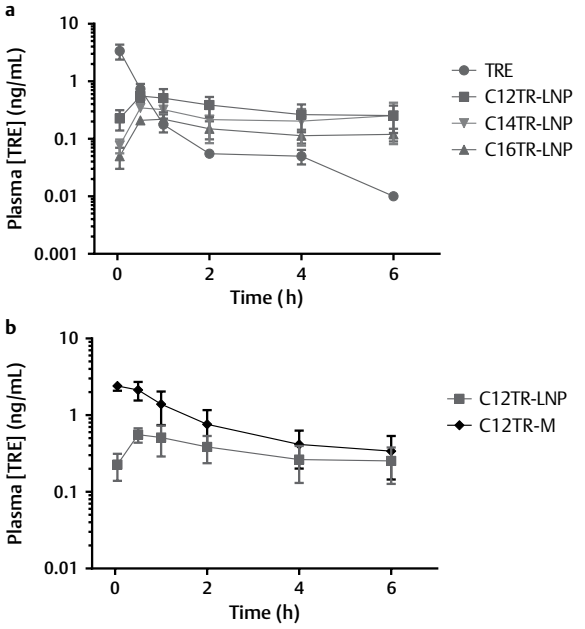

▶ **Fig. 5** Plasma levels of treprostinil (TRE) in rats after administration of TRE or treprostinil prodrug lipid nanoparticles (TPD-LNPs) as a function of time **a** and plasma levels of TRE after administration of LNP versus micellar formulation of dodecyl TRE (C12TR) **b**. Test articles were administered by inhalation to anesthetized ventilated rats over a period of approximately 1 min (Time zero). Dose = 6 ug/kg of TRE equivalent. Each data point represents n = 3. Error bars represent standard deviation.

after about 160 min. Comparatively, rats treated with inhaled C16TR-LNP at equivalent doses to inhaled TRE produced a similar in magnitude but slower reduction in PAP reaching 70 % by 70 min post-dose, which was maintained for the entire duration of the experiment (3 h).

Discussion and Conclusions

This report highlights the initial development of a novel, inhaled, sustained-release formulation of TRE prodrug for treating PAH that provides sustained pulmonary vasodilation. In previous studies a strategy was attempted by which TRE itself was incorporated into a lipid nanoparticle suspension designed to entrap the drug through intermolecular attractions. Treprostinil, an amphiphilic molecule (logP = 4.0) with a terminal carboxyl group that is negatively charged at physiological pH, is chemically compatible for association with lipophilic cationic components known to condense into nanoparticulate structures in the presence of negatively charged molecules [16]. Incorporation of TRE into a lipid nanoparticle comprised of hydrophilic cationic components would hence enable a delayed presentation of TRE as it slowly dissociates from the nanoparticle. A LNP formulation (TRE-LNP) of TRE stemming from this approach was compared against inhaled TRE solution in a pulmonary vasoconstrictive rat model. TRE-LNP demonstrated a somewhat improved pharmacokinetic profile (**Fig. S4a**) relative to inhaled TRE solution, but it failed to sustain the lowering PAP effect (**Fig. S4b**).

To develop a slow-release TRE therapy, we reasoned a 'stronger' association of the drug with the nanoparticle was required and turned to chemical transformation of TRE into a prodrug. A series of TRE prodrugs was made via the acid-catalyzed esterification of TRE in the presence of linear alcohols of varying chain length. They were then packaged into LNPs (▶ **Fig. 1**). The prodrug-nanoparticle strategy added to the delay in TRE release. We speculate that TPD first dissociates from the nanoparticle and then subsequently converts to TRE via endogenous esterases as well as to a small extent via spontaneous hydrolysis before causing vasodilation. This concept is supported by the fact that cAMP activation occurred more rapidly in vitro and TRE was more readily available in plasma when C12TR prodrug was placed into more dynamic micelles as compared to LNPs (▶ **Fig. 4b** and **5b**). TPDs with chain lengths of C8 or longer are stable in vitro when incubated at 37 °C for 24 h (**Fig. S3a**). Thus, enzymatic conversion by esterases is required to present TRE in either in vitro or in vivo experiments. In case of cAMP activation, esterases are likely originating from cell culture. In the

▶ **Table 2** Plasma pharmacokinetic parameters following a single dose of inhaled treprostinil (TRE), dodecyl TRE (C12TR), tetradecyl TRE (C14TR), and hexadecyl TRE (C16TR) lipid nanoparticle (LNP) or micelle (M) delivered by inhalation to anesthetized ventilated rats.

	TRE	C12TR		C14TR		C16TR	
		LNP	M	LNP	M	LNP	M
C_{max} (ng/mL)	3.37	0.56	2.4	0.35	1.20	0.22	0.84
C_{max} (M)/C_{max} (LNP)		4.3	3.4	3.8			
T_{max} (h)	0.05	0.5	0.05	0.5	0.5	1.0	0.5
AUC_{0-6} (ng * h/mL)	1.44	2.06	4.96	1.40	3.66	0.85	2.68
AUC_{0-6}/C_{max} (h)	0.43	3.68	2.07	4.00	3.05	3.86	3.19

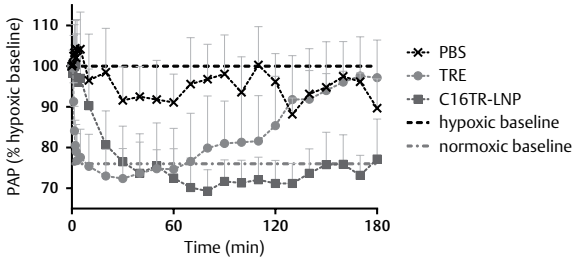

▶ **Fig. 6** Pulmonary arterial pressure response to hypoxic conditions in rats after treatment with phosphate buffered saline (PBS), treprostinil (TRE), and hexadecyl TRE-LNP (C16TR-LNP). Mean pulmonary arterial pressure (PAP) is presented as % relative to hypoxic baseline level. Average hypoxic PAP was 24.2 (SD 2.8) mmHg and average normoxic PAP was 18.4 (SD 2.2) mmHg. Rats were ventilated and dosed by intratracheal inhalation of aerosolized test articles over a period of approximately 1 min (Time zero). Data sets represent n = 6 for PBS, n = 10 for free TRE, and n = 7 for C16TR-LNPs. Estimated pulmonary dose was 6 µg/kg. Error bars represent standard error.

lung tissue, endogenous lung esterases are abundant and can induce quick TPD de-esterification [17, 18]. Of course, to be available for enzymatic conversion, TPDs must first be released from the nanoparticles. One can speculate that this is a diffusion based process and small micelles with greater surface area release TPDs faster than relatively larger LNPs.

The LNP described here serves as a stable carrier of the poorly-soluble TPDs to efficiently disperse the drug in the inhalation solution. The inclusion of the PEGylated lipid Cholesterol-PEG 2000 provided a "stealthy" coating to promote formulation stability in vivo. In addition, a PEGylated shield, along with nanoscale size, contributes to reduced uptake of nanoparticles by macrophages, further providing sustained depot of TPD for release in the lung [19].

The second major factor in achieving sustained presentation of TRE is the nature of the prodrug molecule. In vitro analyses demonstrated a reduced rate of TPD to TRE enzymatic conversion in solution with increasing TPD chain length (**Fig. S3**). One may speculate that the increasing chain length makes the molecule increasingly less compatible with the active site of the esterase mediating TPD to TRE conversion. However, TPD solubility with longer chain length may become too low to accurately measure the conversion, particularly for chain length C12 and longer. This observation was confirmed ex vivo when TPDs were assayed in lung tissue homogenate (▶ **Fig. 3a**). TPDs were added to a final concentration of only 200 nM, small enough to remain soluble in presence of lung homogenate. As hydrophobic derivatives, TPDs likely associate with various proteins and cell bilayer structures. This in turn may affect the observed TPD conversion. One may argue that this is more relevant to in vivo TPD metabolism when they are delivered to the lung. TPD conversion rate varied greatly between different chain length prodrugs (▶ **Table 1**). C14TR was the slowest converting measured prodrug at about 1 % per hour, and C16TR conversion was not detected. These results likely underestimate actual conversion rate in vivo as the lung homogenate was diluted approximately 5-fold. The homogenization process may also break cells, releasing proteases and other enzymes and thus reduce activity of esterases. Nonetheless, it allowed narrowing of the list of potential TPD candidates that are able to provide 24 h release of TRE to C12TR, C14TR, and C16TR.

The difference in observed conversion rates in different species was noted, with dog being the fastest converting and monkey being the slowest. It is not clear how this will translate into humans considering the report by Berry et al. presenting the activity of three major classes of esterases (carboxylesterase, butyryl-cholinesterase, and paraoxonase) [20]. Substantial species differences in activity of these esterases were observed between the mouse, rat, dog monkey and human, and those differences depended in turn on the substrate and the tissue studied. For example, carboxylesterase was most active in rat plasma and liver, while monkeys showed moderate activity in liver, and dogs had low or no activity in both plasma and liver. Butyryl-cholinesterase, on the other hand, was most active in monkey plasma and moderately active in dog plasma but not in liver. One might speculate that conversion in humans may be similar to monkey (primate), i. e., slower than in dog or rat.

When TPD-LNPs were evaluated in vitro in modified CHO-K1 cells, where cAMP levels were used as a measure of TRE receptor activation, the data similarly showed reduced activation rates with increasing TPD chain length (▶ **Fig. 4a**), an observation that was congruent with the lung homogenate conversion data. Here too, TPD must first dissociate from the LNP and get converted to TRE by esterases. Longer chain TPDs likely exhibit both reduced release from LNP and reduced enzymatic conversion rates. The enzymatic conversion is required for the activity as it was shown in a separate study that the prodrugs are inactive towards the prostacyclin receptor [21]. Also, in a study using a non-metabolizable version of the prodrug (ether linkage replaced the ester linkage in the prod-

rug) the compound demonstrated no pulmonary vasodilation in a rat model [21].

One may speculate whether enzymatic conversion of TPD occurs intra- or extracellularly. TPD is a neutral hydrophobic molecule with low solubility in water but good affinity to lipid bilayers (data not shown). It can exchange between LNP and cell plasma membranes, then further translocate inside the cells. TRE, in turn, is highly soluble in water when deprotonated at neutral pH but due to weak acidity of the carboxylic group can also easily permeate biological membranes, as evident from the TRE PK profile. Thus, both TPD and TRE can likely be present extra- and intracellularly.

Rat PK data further confirms sustained supply of TRE when delivered as TPD-LNP intratracheally to anesthetized ventilated rats (▶ **Fig. 5a** and ▶ **Table 2)**. Inhaled C12TR, C14TR, and C16TR TPD-LNPs all exhibited greatly reduced C_{max} relative to inhaled TRE solution in ventilated rats. However, $AUC_{0\text{-}6}$ was comparable or higher than with TRE solution, due to sustained TRE plasma levels in rats dosed with TPD-LNPs. Again, we observed a trend with longer chain prodrugs producing lower C_{max} than the shorter chain ones, suggesting slower conversion rate.

Comparison of the PK profile resulting from dosing with C12TR in nanoparticle and in micellar form once more confirms the role of slow release of C12TR from LNPs: TRE plasma C_{max} was lower and reached later after administration of TPD-LNPs compared to TPD-Micelle formulation (▶ **Fig. 5b**). These observations are in line with the expectation that micelles, which were measured to be 13 nm in size, provide greater surface area and more readily supply TPDs to be converted by esterases to TRE. LNPs are larger in size (100 nm) and could release TPDs slower due to a lower surface area.

Finally, the sustained levels of plasma TRE stemming from TPD-LNP formulations were linked to drug activity in a rat model of hypoxia-induced pulmonary vasoconstriction. In ▶ **Fig. 6**, the data demonstrate that C16TR-LNP provides a sustained reduction in PAP to normoxic levels. The effect observed for C16TR-LNP was longer lasting within the time-frame of the experiment as compared to TRE or shorter chain prodrugs (data not shown). Here, rats were surgically prepared for intratracheal ventilation and inhalation dosing, and the pulmonary artery was catheterized for PAP measurements. Typically, the duration of experiment in these settings is limited to a reliable PAP recording of up to 3 h or so. The available PK data suggest though that a longer in vivo efficacy study may prove sustained effect lasting long enough to be a viable therapeutic candidate.

We have developed and evaluated an inhaled novel, slow-release, nanoparticle-formulated prodrug of TRE intended for the treatment of PAH that may address pitfalls associated with current clinically used forms of TRE. The most promising candidate formulation, C16TR-LNP has a reduced C_{max} compared to inhaled solution TRE while maintaining a therapeutic extended vasodilatory effect in a rat hypoxia model of pulmonary vasoconstriction. The observed kinetics can be attributed to a delay in TRE presentation which is dictated by TPD dissociation from the nanoparticle and conversion to the active TRE in vivo. These results support that further development of C16TR-LNP as a possible therapy to treat PAH is warranted.

Acknowledgements

The authors would like to thank Paul J. Klecha, Consuelo Garcia, and Dr. Tara E. Henn for assisting with the formulation and physiochemical characterization of TPDs and TPD-LNPs and Dr. Jane Ong for in vitro evaluation of these compounds and formulations. The authors would also like to thank Dr. Keith DiPetrillo for his valuable thoughts and contribution in preparing this manuscript. Funding for this work was provided by Insmed Incorporated (Bridgewater, NJ).

The authors meet criteria for authorship as recommended by the International Committee of Medical Journal Editors (ICMJE), were fully responsible for all content and editorial decisions, and were involved at all stages of manuscript development.

Conflict of Interest

All authors of this work as well as the work presented in this manuscript were funded by Insmed Incorporated.

References

[1] Tyvaso Patient Package Insert. 2013

[2] Nadler ST, Edelman JD. Inhaled treprostinil and pulmonary arterial hypertension. Vasc Health Risk Manag 2010; 6: 1115–1124

[3] Gessler T, Seeger W, Schmehl T. The potential for inhaled treprostinil in the treatment of pulmonary arterial hypertension. Therapeutic Advances in Respiratory Disease 2011; 5: 195–206

[4] McGoon MD, Benza RL, Escribano-Subias P et al. Pulmonary arterial hypertension: epidemiology and registries. J Am Coll Cardiol 2013; 62: D51–D59

[5] LeVarge BL. Prostanoid therapies in the management of pulmonary arterial hypertension. Ther Clin Risk Manag 2015; 11: 535–547

[6] Sitbon O, Morrell N. Pathways in pulmonary arterial hypertension: the future is here. Eur Respir Rev 2012; 21: 321–327

[7] Whittle BJ, Silverstein AM, Mottola DM et al. Binding and activity of the prostacyclin receptor (IP) agonists, treprostinil and iloprost, at human prostanoid receptors: treprostinil is a potent DP1 and EP2 agonist. Biochem Pharmacol 2012; 84: 68–75

[8] Olschewski H, Simonneau G, Galiè N et al. Inhaled Iloprost for Severe Pulmonary Hypertension. The New England Journal of Medicine 2002; 347: 322–329

[9] Simonneau G, Barst RJ, Galie N et al. Continuous Subcutaneous Infusion of Treprostinil, a Prostacyclin Analogue, in Patients with Pulmonary Arterial Hypertension. Am J Respir Crit Care Med 2002; 165: 800–804

[10] Remodulin Patient Package Insert. 2014

[11] deLartigue J. Oral treprostinil for treatment of pulmonary arterial hypertension. Drugs of Today 2014; 50: 557–565

[12] Orenitram Patient Package Insert. 2014

[13] Malinin V, Li Z, Chapman RW et al. Treprostinil Pharmacokinetics in Rats Are Extended Using Inhaled Prodrug Formulations, in European Respiratory Society International Congress. 2014 Munich: Poster 2367

Shein-Chung C, Liu J-p. Design and Analysis of Bioavailability and Bioequivalence Studies. 3rd ed., Chapman & Hall / CRC Biostatistics Series, New York: CRC Press, 2008: 24–29

[14] Li Z , Chapman RW, Malinin VS et al. Inhaled INS1009 Demonstrates Localized Pulmonary Vasodilation, in European Respiratory Society International Congress. 2016 London, UK: Poster: PA2485

[15] Zhu L, Mahato RI. Lipid and polymeric carrier-mediated nucleic acid delivery. Expert Opin Drug Deliv 2010; 7: 1209–1226

[16] McCracken NW, Blain PG, Williams FM. Nature and role of xenobiotic metabolizing esterases in rat liver, lung, skin and blood. Biochemical Pharmacology 1993; 45: 31–36

[17] Basu A, Glew RH, Evans RW et al. Isolation and characterization of a fatty acyl esterase from rat lung. Archives of Biochemistry and Biophysics 1988; 261: 384–393

[18] Walkey CD, Olsen JB, Guo H et al. Nanoparticle size and surface chemistry determine serum protein adsorption and macrophage uptake. J Am Chem Soc 2012; 134: 2139–2147

[19] Berry LM, Wollenberg L, Zhao Z. Esterase Activities in the Blood, Liver and Intestine of Several Preclinical Species and Humans. Drug Metabolism Letters 2009; 3: 70–77

[20] Corboz MR, Li Z, Malinin VS et al. Preclinical Pharmacology and Pharmacokinetics of Inhaled Hexadecyl-Treprostinil (C16TR), a Pulmonary Vasodilator Prodrug. Journal of Pharmacology and Experimental Therapeutics 2017; 363: 348–357